Tree Genetics & Genomes (2018) 14: 91
https://doi.org/10.1007/s11295-018-1304-7

ORIGINAL ARTICLE

Linkage and association analysis of dihydrochalcones phloridzin, sieboldin, and trilobatin in *Malus*

Benjamin L. Gutierrez[1,2] · Jie Arro[2] · Gan-Yuan Zhong[2] · Susan K. Brown[1]

Received: 25 July 2018 / Revised: 26 October 2018 / Accepted: 12 November 2018 / Published online: 23 November 2018

Abstract

Dihydrochalcones (DHCs) are a distinctive characteristic of *Malus* species, with phloridzin as the major DHC in most *Malus* species, including cultivated apple. DHCs in apple have unique chemical properties with commercial and nutritional value and may yield important insights into the evolution and physiology of apple. A few species produce sieboldin and trilobatin instead of phloridzin, and interspecific hybridization produce offspring with combinations of phloridzin, sieboldin, and trilobatin. Using *Malus prunifolia* PI 89816 as a common male parent, five F_1 populations were developed to understand the genetic basis of these DHCs in *Malus*. We measured DHC content in each population and observed segregation into five distinct DHC profiles, which fit a model for three independently segregating loci. QTL associated with DHC content were identified on linkage groups 7 and 8 of the *Malus* genome using linkage analysis with a cross of NY-152 by *M. prunifolia* PI 589816 and association mapping with a *Malus* germplasm collection. In addition to DHC segregation, we observed variation in the relative proportions of phloridzin, sieboldin, and trilobatin. The QTL identified represent a critical step in understanding the genetic controllers of DHC content in *Malus*.

Keywords Apple · Dihydrochalcone (DHC) · Genetic mapping · Genotyping-by-sequencing (GBS) · *Malus* · Phloridzin · Quantitative trait loci (QTL)

Background

Apples are a high-value food crop with unique nutritional qualities, stemming primarily from production of phenolic compounds. Flavonoids, a class of phenolics, contribute significantly to the color and nutritional value of apple, of which dihydrochalcones (DHCs) are a minor subclass. Contrasted with the diversity of phenolic compounds (thousands described), approximately 256 DHCs have been described in a wide distribution of plant species, though few are isolated from edible plants (Rivière 2016). Despite the rarity of DHCs, they are abundant in *Malus* species, and can represent up to 90% of the phenolic profile and 14% of the leaf dry weight (Gosch et al. 2010b). DHCs are absent or produced only in trace amounts in other food crops, including relatives within the Rosaceae. Phloridzin (phloretin 2′-*O*-glucoside) is the prominent dihydrochalcone in *Malus* species, including cultivated apple, and has anti-diabetic effects through increased insulin sensitivity and inhibition of sodium glucose cotransporter-2 (SGLT-2) (Najafian et al. 2012). Additionally, phloridzin has antioxidant, anti-cancer, anti-inflammatory, and phytoestrogenic effects (Puel et al. 2005; Nair et al. 2014). In a few *Malus* species, phloridzin content is replaced entirely by phloretin derivatives, sieboldin (3-hydroxyphloretin-4′-*O*-glucoside), and trilobatin (phloretin-4′-*O*-glucoside), which also have unique chemical properties. Higher antioxidant activity was observed in sieboldin relative to phloridzin and trilobatin, with a capacity to inhibit vasoconstriction and formation of advanced glycation end products associated with several degenerative diseases (Dugé de

Communicated by M. Troggio

Electronic supplementary material The online version of this article (https://doi.org/10.1007/s11295-018-1304-7) contains supplementary material, which is available to authorized users.

✉ Benjamin L. Gutierrez
ben.gutierrez@ars.usda.gov

[1] Plant Breeding and Genetics Section, School of Integrative Plant Science, NYSAES, Cornell University, 630 W. North St., Geneva, NY 14456, USA

[2] United States Department of Agriculture-Agricultural Research Service, Plant Genetic Resources Unit, 630 W. North St., Geneva, NY 14456, USA

Bernonville et al. 2010; Xiao et al. 2017). Trilobatin, a sweet DHC, has anti-diabetic effects differing from phloridzin through α-glucosidase inhibition instead of SGLT-2 and reduction of chronic inflammation related to lipopolysaccharides (Dong et al. 2012; Fan et al. 2015). Trilobatin is about 300 times sweeter than sucrose, with potential as a naturally occurring commercial sweetener (Rivière 2016). Phloretin, the aglycone precursor to these DHCs, also has potential industrial value and nutritional quality, although it is found in lower concentrations (Behzad et al. 2017). Figure 1 depicts the synthesis of phloretin, phloridzin, sieboldin, and trilobatin.

DHCs have been implicated in disease resistance in *Malus*, although there is no conclusive evidence directly relating DHC concentrations to resistance (Mikulič Petkovšek et al. 2008; Dugé de Bernonville et al. 2011). Fluctuations in DHC and flavonoid biosynthesis in response to infection were reported (Slatnar et al. 2012; Gaucher et al. 2013). Gosch et al. (2009) proposed that DHCs contribute to disease resistance through an oxidative cascade, and Gaucher et al. (2013) and Hutabarat et al. (2016) observed variation in this cascade in susceptible and resistant genotypes. Conversely, DHCs have been associated with apple replant disease by signaling and promoting pathogen growth (Yin et al. 2017). Phloridzin may act as an auxin regulator in *Malus* (Dare et al. 2017). Independent RNA interference silencing of chalcone synthase and phloretin-glycosyltransferases resulted in reduced auxin transport and aberrant tree architecture in apple (Dare and Hellens 2013; Dare et al. 2017). Whether or not sieboldin and trilobatin serve similar roles in *Malus* species needs to be researched.

While most *Malus* species produce phloridzin as the primary DHC, *Malus toringo* (Siebold) Siebold ex de Vriese and *Malus sargentii* Rehder replace phloridzin with sieboldin, and *Malus trilobata* (Poir.) Schneid. replaces phloridzin with trilobatin (Williams 1961). Interspecific hybridization with these species and other *Malus* species results in codominant inheritance of phloridzin, sieboldin, and trilobatin (Williams and Jarrett 1975; Hunter 1975). Williams and Jarrett (1975) first suggested DHCs in apple were controlled by independently segregating genes. Unlike other phenolics, with well-characterized metabolic networks, little is known about DHC synthesis and regulation. Its unique presence in cultivated apple has made apple somewhat of a model for DHCs. Most genetic studies in apple involve F_1 progeny from single or multiple families (McClure et al. 2016). Advances in genotyping allow analysis of diverse germplasm through association studies, though this approach remains challenging in apple due to low linkage disequilibrium related to high heterozygosity and obligate outcrossing, and large populations required to detect small effect QTL (Kumar et al. 2013; McClure et al. 2014). QTL for several major apple phenolics have been reported, including a few minor, but no major QTL related to phloridzin content variation (Chagné et al. 2012; Khan et al. 2012; Verdu et al. 2014). More research is needed to understand the interactions of DHC metabolic pathways.

The aim of this study was to better characterize the genetic controllers of dihydrochalcone content in apple, particularly, those controlling sieboldin and trilobatin. We followed the segregation of major apple DHCs phloridzin, sieboldin, and trilobatin in five apple F_1 populations and confirmed that DHCs segregate independently using chi-square analysis. Using linkage and association mapping, we identified marker-trait associations on apple linkage groups 7 and 8.

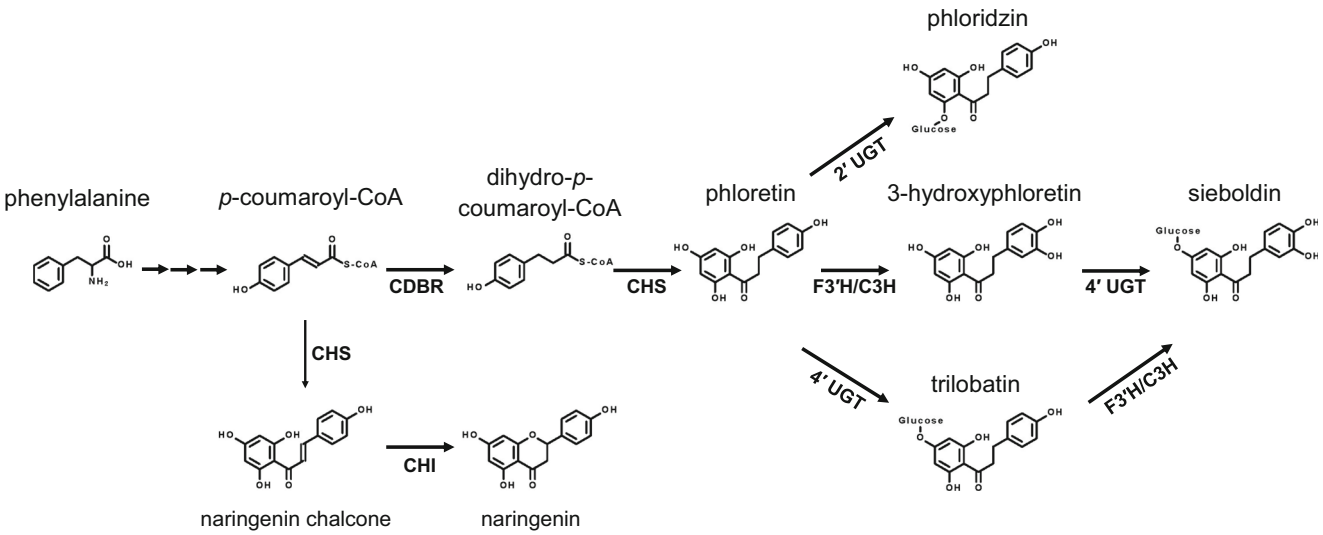

Fig. 1 Proposed synthesis of the dihydrochalcones phloretin, phloridzin, trilobatin, and sieboldin. Carbon double bond reductase (CDBR), chalone-3-hydroxylase (C3H), chalcone isomerase (CHI), chalcone synthase (CHS), flavonoid 3′-hydroxylase (F3′H), UPD-dependent glycosyltransferase (UGT)

Materials and methods

Plant material

Five F_1 populations were developed using *Malus prunifolia* (Willd.) Borkh. PI 589816 as the pollen parent. Seed parents included the ornamental cultivar 'Evereste' (population 16,705) and selections from the Cornell University apple breeding program in Geneva, NY; NY-152 ('Wijcik McIntosh' × 'Suncrisp'|) (population 13,427), and three 'Evereste'× 'Red Jade' progeny (populations 16,708, 16,709, and 16,710) (Table 1). Pedigrees are illustrated in Supplemental Fig. 1. *M. prunifolia* PI 589816, 'Evereste', and the 'Evereste' × 'Red Jade' progeny were selected based on dihydrochalcone profiles, containing phloridzin, sieboldin, and trilobatin. Population 13,427 was initially developed to study the columnar habit of NY-152. Each cross had high fruit set and seed viability (> 95%), although both PI 589816 and NY-152 are pale green lethal carriers and 25% of the initial seedlings died at the cotyledon stage in population 13,427 (Orcheski et al. 2015). Population 13,427 was from a cross made in 2013, germinated in the summer of 2015, overwintered in a greenhouse, and planted in spring of 2016. Leaf samples of 13,427 were collected from the greenhouse (fall 2015) and from the field (fall 2016). Populations 16,705, 16,708, 16,709, and 16,710 were developed in 2016, stratified in the winter of 2017, and planted in spring 2017. Samples were collected from the parents for HPLC and DNA extraction. Population 13,427 was evaluated for morphological traits including plant height, architecture, and internode length, all related to the columnar phenotype. A major QTL for columnar was identified previously on linkage group 10 (Morimoto and Banno 2015) and used to validate maps in population 13,427. PI 589816 and 'Red Jade' (PI 588786) are maintained on 'EMLA 7' rootstock in the USDA-ARS National Plant Germplasm System (NPGS) *Malus* collection in Geneva, NY. 'Evereste', NY-152, and 'Evereste' × 'Red Jade' selections are maintained on 'Geneva 935' rootstock. Leaf samples from 377 diverse accessions were collected from the NPGS *Malus* collection from 2013 to 2015 (Gutierrez et al. 2018).

High performance liquid chromatography

Phenolics were extracted from mature leaf samples following the methods described by Gutierrez et al. (2018). Briefly, 25 mg of ground leaf tissue was suspended in 1.5 ml of 70% methanol (99.9%) with 2% formic acid (98–100%) for 10 min then centrifuged, with two technical replicates per genotype. Supernatant was filtered with a 0.20-μm syringe filter, and compounds were separated with an Inertsil ODS-3 column (4.6 × 250 mm; 5 μm, GL Sciences Inc., Tokyo, Japan) and 15% acetonitrile, 10% formic acid mobile phase at 1 mL/min on a Hitachi LaChrom Elite (San Jose, CA, USA) liquid chromatograph equipped with diode array detector. Standard curves for phloridzin, sieboldin, and trilobatin ranged from 7.8 μg to 1000 μg with $R^2 > 0.99$, and sample values expressed in milligram per gram leaf fresh weight.

Genotyping

Individuals of population 13,427 were scored using genotyping-by-sequencing (Elshire et al. 2011) following the methods described previously (Gutierrez et al. 2018). Sequence tags were aligned to the *M. domestica* Whole Genome Reference Assembly v.2 (https://www.rosaceae.org/) using Bowtie 2 (Langmead and Salzberg 2012) with parameters D, R, N, L and *i* set to 30, 5, 1, 15, and S, 1, 0.25 to reduce misalignment. The Tassel 5 (Glaubitz et al. 2014) GBS pipeline was used for SNP calling. Ten replicates of parents NY-152 and PI 589816 were merged into single genotypes. VCFtools (Danecek et al. 2011) was used to filter data; twenty-six individuals were removed for low mean depth; sites were filtered for read depth of 8 and minor allele frequency of 0.20; and genotypes were filtered for 80% missing data. Kinship analysis and PCA identified twenty-five potentially outcrossed individuals which were removed from subsequent analyses. Genotypes were filtered based on Mendelian error calculated in PLINK 1.9 (Purcell et al. 2007) and set to missing. SNP markers were filtered based on chi-square tests for segregation distortion and > 0.95 similarity using JoinMap4.1. Genotypes from 280 of *Malus* germplasm accessions included in this study were scored previously (Gutierrez et al. 2018). Data included 274 individuals with mean depth above 18 (15th percentile) and 51,348 SNPs filtered for < 20% missing data, read depth of 10, minor allele frequency of 0.10, and QC > 98. LinkImpute (Money et al. 2015) was used to impute missing genotypes with parameters *l* and *k* set to 5 and 20.

Genetic maps and QTL analysis

GBS markers were divided into male (<nnxnp>) and female (<lmxll>) subsets based on JoinMap 4.1 (Kyazma, NL) conventions. Genetic maps for each parent were constructed with JoinMap 4.1, using regression mapping with linkages with recombination frequencies < 0.35 and LOD > 1.0, a jump threshold of 5.0 and Kosambi's function. Loci were iteratively added to linkage groups based on strongest cross-link value. Interval mapping with regression analysis was done for each map separately using MapQTL 6 (Kyazma, NL) software. Significance threshold for each trait was determined through permutations test ($n = 10{,}000$). Association mapping was performed using the mixed linear model (MLM): $\mathbf{Y} = \mathbf{X}\boldsymbol{\beta} + \mathbf{Z}\mathbf{u} + \mathbf{e}$, where $\mathbf{Y}$ is a vector of DHC ratios; $\mathbf{X}$ and $\mathbf{Z}$ are design matrices; $\boldsymbol{\beta}$ is a fixed effects vector, which includes SNP markers, population structure (Q) determined by the first three

Table 1 Pedigree, parental dihydrochalcone classes, and population size for each F_1 population

Population	Parents	DHC profile	Count
13,427	NY-152 ('Wijcik McIntosh' × 'Suncrisp') × PI 589816	P × SPT	445
16,705	'Evereste' × PI 589816	SPT × SPT	150
16,708	00121–005 ('Evereste' × 'Red Jade') × PI 589816	SPT × SPT	81
16,709	00121–063 ('Evereste'× 'Red Jade') × PI 589816	SPT × SPT	44
16,710	00121–016 ('Evereste' × 'Red Jade') × PI 589816	SPT × SPT	151

principal components, and the model intercept; **u** is a vector of random additive genetic effects with covariance matrix $\mathbf{2\,K}\sigma_a^2$, where **K** is a VanRaden kinship matrix **(K)** determined by SNP markers; **X** and **Z** are design matrices; and **e** are the residual effects (Wang et al. 2014). MLM was implemented in GAPIT (Lipka et al. 2012).

Data analysis

Principal component analysis and statistical tests, including chi-square tests for goodness of fit and independence, Pearson correlations, and ANOVA tests were calculated in R 3.3.2 (R Core Team 2016). Welch's ANOVA and Games-Howell post hoc tests were used where sample size was unequal or equal variance could not be assumed, based on Bartlett's and Levene's tests for homogeneity of variance. Games-Howell tests were calculated in R package "userfriendlyscience" (Peters 2018). Mosaic plots and Pearson residuals were calculated using R package "vcd" (Zeileis et al. 2007).

Results

Dihydrochalcone content in F_1 populations

DHCs were measured in all populations and their parents. Mean retention times across all samples for sieboldin, phloridzin, and trilobatin were 15.0, 20.3, and 30.7 min, respectively. Mean DHC content for parents of each population is presented in Table 2. Sieboldin was not observed independent of trilobatin in the progeny nor in the *Malus* germplasm (Gutierrez et al. 2018), though the proportion of sieboldin to trilobatin can be large with trilobatin detected in trace amounts.

DHC genotypes of parents were inferred according to a three loci model and reported using codes *A* (phloridzin), *B* (trilobatin), and *C* (sieboldin) for simplicity. PI 589816 (SPT) is heterozygous for phloridzin, sieboldin, and trilobatin (*AaBbCc*), based on segregation in all five populations. NY-152 (P) is homozygous for phloridzin, and recessive for sieboldin, and trilobatin (*AAbbcc*), based on 1:2:1 segregation for PT, P, and SPT in population 13,427. 'Evereste' (SPT) is homozygous for phloridzin and sieboldin, and heterozygous for trilobatin (*AABbCC*), based on 3:1 segregation of SPT and P in population 16,705. In population 16,708, five DHC profiles were observed; P, T, PT, ST, and SPT, and selection 00121-005 was presumed to be heterozygous for phloridzin, sieboldin, and trilobatin (*AaBbCc*). Selections 00121-063 (SPT) and 00121-016 (SPT) are homozygous for phloridzin and heterozygous for sieboldin and trilobatin (*AABbCc*), based on the 9:4:3 ratio of SPT, P, and PT in populations 16,709 and 16,710. Progeny DHC profiles suggest they are controlled by three independently segregating loci (Williams and Jarrett 1975) as determined by a chi-square goodness of fit test ($p > 0.05$) (Fig. 2; Table 3). However, population 16,708 deviated significantly from expected ratios (χ^2 (5) = 52.3, $p < 0.001$). Expected values were calculated from inferred genotypes, with the assumption that unobserved SP types of genotypes *A_bbC_* manifest as P types.

DHC content varied significantly within and among populations, based on Welch's one-way analysis of variance and Games-Howell post hoc tests with Bonferroni correction.

Table 2 Mean leaf dihydrochalcone content (mg/g) in parents of apple F_1 populations

Parent	DHC profile	Hypothetical genotypes	Phloridzin	Sieboldin	Trilobatin	Total DHC
PI 589816	SPT	*AaBbCc*	53.8	17.2	7.4	78.3
'Evereste'	SPT	*AABbCC*	33.6	30.2	5.5	69.2
'Red Jade'	P	*Aabbcc*	90.5	n.d	n.d	90.5
NY-152	P	*AAbbcc*	37.3	n.d	n.d	37.3
00121-005	SPT	*AaBbCc*	21.0	0.8	1.5	23.3
00121-063	SPT	*AABbCc*	27.1	20.7	20.4	68.3
00121–016	SPT	*AABbCc*	20.9	5.6	7.3	33.8

n.d., not detected

Phloridzin content (11.5 to 144.3 mg/g) was significantly different among populations ($F(4,170) = 9.35$, $p < 0.001$). Sieboldin content (3.1 to 57.9 mg/g) varied among populations ($F(4, 77) = 55.98$, $p < 0.0001$), and was significantly lower in population 13,427. Trilobatin content (0.1 to 46.5 mg/g) was different among populations ($F(4, 103.9) = 138.6$, $p < 0.0001$) and was significantly lower in population 16,705. Total DHC (15.8 to 144.3 mg/g) and varied significantly among populations ($F(4, 6.9) = 34.4$, $p < 0.001$). Mean and range of individual and total DHC content are listed by population in Table 4 and depicted in Supplemental Fig. 2. In population 13,427, mean DHC content was higher in 2016. This was likely due to environmental variation from greenhouse samples in 2015 to field samples in 2016.

Individual DHC content varied by DHC profiles. Mean phloridzin content was higher in P profiles than in PT or SPT ($F(2, 1284.5) = 423.56$, $p < 0.0001$) and mean trilobatin content was higher in PT profiles than in SPT (t (1), $p < 0.0001$), consistent across all populations (Supplemental Fig. 3). Correlations among individual DHCs varied by population. In 13,427, there is a moderate correlation between sieboldin and phloridzin ($r = 0.54$), trilobatin and phloridzin ($r = 0.52$), and trilobatin and sieboldin ($r = 0.50$), where $p < 0.0001$. When subset by DHC profiles PT and SPT in population 13,427, the correlations between trilobatin and phloridzin are 0.74 and 0.71, respectively. Plotting trilobatin by phloridzin reveals two distinct groups based on dihydrochalcone profile (Supplemental Fig. 4). This pattern was not observed in other populations. There was a moderate correlation between phloridzin and sieboldin ($r = 0.62$, $p < 0.001$) in population 16,708 and between sieboldin and trilobatin ($r = 0.52$, $p < 0.0001$) in population 16,710. Other correlations among DHCs in these populations varied from weak to moderate but were not significant ($p > 0.01$).

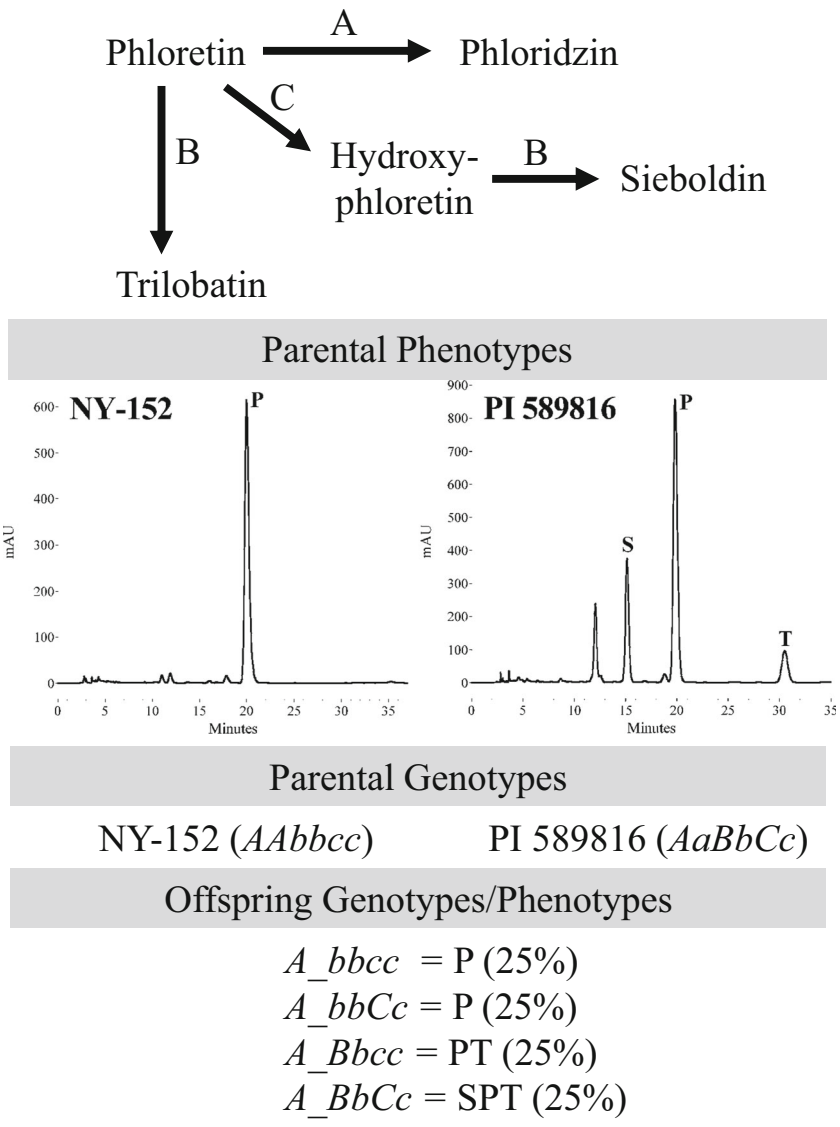

Fig. 2 Three-gene codominant model for phloridzin, sieboldin, and trilobatin segregation in population 13,427. Loci *A*, *B*, and *C* result in synthesis of phloridzin, trilobatin, and sieboldin, respectively, where sieboldin synthesis is dependent upon *B* allele (*A_bbC_* produces only phloridzin). Loci presumed to be unlinked based on segregation ratios. NY-152 produces only phloridzin (P), and PI 589816 produces phloridzin, sieboldin, and trilobatin (SPT)

Table 3 Number of offspring in each DHC profiles by population and *Malus* germplasm from Geneva, NY. Chi-square goodness of fit test based on inferred parental genotypes

Population	DHC profiles					Parental profiles	Hypothetical parental genotypes	Chi-square value (df, *p* value)
	P	T	PT	ST	SPT			
13,427	214	0	109	0	97	P × SPT	*AAbbcc* × *AaBbCc*	0.8 (2, 0.66)
16,705	36	0	0	0	114	SPT × SPT	*AABbCC* × *AaBbCc*	0.1 (1, 0.77)
16,708	39	2	3	6	31	SPT × SPT	*AaBbCc* × *AaBbCc*	52.3 (5, < 0.0001***)
16,709	14	0	9	0	21	SPT × SPT	*AABbCc* × *AaBbCc*	1.5 (2, 0.48)
16,710	41	0	34	0	76	SPT × SPT	*AABbCc* × *AaBbCc*	2.7 (2, 0.26)
Germplasm[a]	284	1	2	36	54			

[a] Gutierrez et al. 2018

***$p < 0.001$

The relative proportions of phloridzin, sieboldin, and trilobatin varied across populations. Phloridzin was the prominent DHC in all populations, with mean proportions > 60%. In population 13,427 phloridzin was the prominent DHC in all individuals, ranging from 64 to 87% of the total content in SPT profiles. A few individuals in the other populations had proportions of sieboldin and trilobatin > 50% and as high as 64%. Except for rare T profiles, trilobatin was generally a minor component in all five populations. The proportions of phloridzin, sieboldin, and trilobatin in progeny with PT and SPT profiles are presented in Table 5.

Genetic mapping

GBS produced 1,115,484 reads, 37.9% of which aligned uniquely to the reference genome, and 15.7% aligned > 1 time. After filtering, ~3100 and 1500 GBS markers were available for the male and female maps, respectively. Genetic maps were validated by mapping columnar architecture to linkage group (LG) 10 (Morimoto and Banno 2015) using plant height, internode length, and tree architecture descriptors. Interval mapping using the male genetic map identified a QTL on the bottom of LG 7 near marker LG7_27346079 at 67.1 cM, which explained 24.9, 22.4, and 50.2% of the variation of phloridzin, sieboldin, and trilobatin content, respectively. Another QTL on the bottom of LG 8 near marker LG8_33717934 at 63.7 cM explained 19.8% of the variation in sieboldin content. Male genetic maps of linkage groups 7 and 8 are highlighted in Fig. 3. Figure 4 illustrates the proportions of DHCs with the two most significant SNP markers associated with trilobatin and sieboldin content. Marker LG7_27743464 follows a 1:1 segregation between homozygous G and profile P, and heterozygous A/G and profiles PT and SPT. This marker is likely associated with trilobatin synthesis in this population, representing the *B* allele used in inferred parental genotypes. Marker LG8_31717934, associated with sieboldin synthesis, represents the *C* allele in inferred genotypes. Nearly all SPT profiles are heterozygous (C/T) at this locus, while most PT and over half P profiles are homozygous (C/C). About 40% of individuals of profile P also are heterozygous (C/T) for marker LG8_31717934, which suggests that predicted SP profiles manifest as P.

Within the *Malus* germplasm collection, we identified an association (Fig. 5) around the same position on LG 7 related to dihydrochalcone composition of 279 individuals. Marker LG7_27704634 homozygous G/G was tightly associated with profile P, whereas a significant portion of SPT, PT, and ST profiles was heterozygous G/T or homozygous T/T.

Discussion

DHC profiles observed in these populations followed a pattern of three codominantly expressed, segregating loci. Chi-square

Table 4 Mean and range of leaf dihydrochalcone content (mg/g) in apple F_1 populations

Population	Date	Phloridzin		Sieboldin		Trilobatin		Total DHC	
		Mean ± sd	Range	Mean ± sd	Range	Mean ± sd	Range	Mean ± sd	Range
13,427	2015	50.6 ± 14.1	18.1–106.2	10.7 ± 3.0	3.9–19.7	12.4 ± 6.2	3.2–27.4	58.7 ± 13.8	20.3–106.2
13,427	2016	69.2 ± 20.5	25.6–133.3	10.0 ± 3.8	4.1–20.1	15.0 ± 6.9	2.7–33.9	78.3 ± 16.4	33.5–133.3
16,705	2017	51.3 ± 23.6	16.3–144.3	20.4 ± 9.7	5.1–46.0	3.2 ± 3.4	0.1–19.4	69.1 ± 19.9	34.0–144.3
16,708	2017	58.2 ± 26.3	2.5–130.1	22.9 ± 12.1	5.7–57.9	10.9 ± 10.5	0.3–37.9	68.6 ± 22.4	19.8–130.1
16,709	2017	55.2 ± 22.1	24.8–104.5	19.4 ± 8.7	5.5–34.0	15.7 ± 12.2	2.9–46.5	75.1 ± 17.8	39.6–104.5
16,710	2017	47.5 ± 19.6	11.5–97.9	14.9 ± 7.9	3.1–39.1	11.5 ± 8.4	1.0–36.7	63.5 ± 16.3	15.8–111.7

Table 5 Mean (range) of leaf dihydrochalcone proportions of apple F_1 populations with PT and SPT profiles

Population	PT profiles		SPT profiles		
	P/total DHC	T/total DHC	P/total DHC	S/total DHC	T/total DHC
13,427	0.72 (0.63–0.88)	0.27 (0.12–0.37)	0.73 (0.64–0.87)	0.15 (0.06–0.23)	0.12 (0.05–0.20)
16,705	n.d.	n.d.	0.63 (0.37–0.88)	0.31 (0.11–0.62)	0.05 (<0.01–0.25)
16,708	0.60 (0.54–0.63)	0.40 (0.37–0.46)	0.60 (0.48–0.78)	0.31 (0.12–0.57)	0.11 (<0.01–0.43)
16,709	0.60 (0.36–0.87)	0.40 (0.13–0.64)	0.61 (0.42–0.75)	0.25 (0.12–0.37)	0.13 (0.04–0.30)
16,710	0.66 (0.37–0.84)	0.34 (0.15–0.63)	0.63 (0.38–0.88)	0.24 (0.05–0.50)	0.12 (0.03–0.29)

n.d., not determined

tests for goodness of fit in all populations but 16,708 suggest these loci are unlinked. It is unclear why population 16,708 deviated significantly from the other populations. Selection 00121-005 was unique among the other 'Evereste' × 'Red Jade' selections, with reduced levels of sieboldin and trilobatin (Table 2). Additionally, it has unique morphological characteristics, including linear to lanceolate leaf shape, generally < 7-mm-wide and 28-mm-long leaves, shortened internodes (< 12.5 mm). Supplemental Fig. 5 highlights leaf variation between population founders. There are potentially other genetic factors affecting DHC concentrations in this population, which merit further investigation.

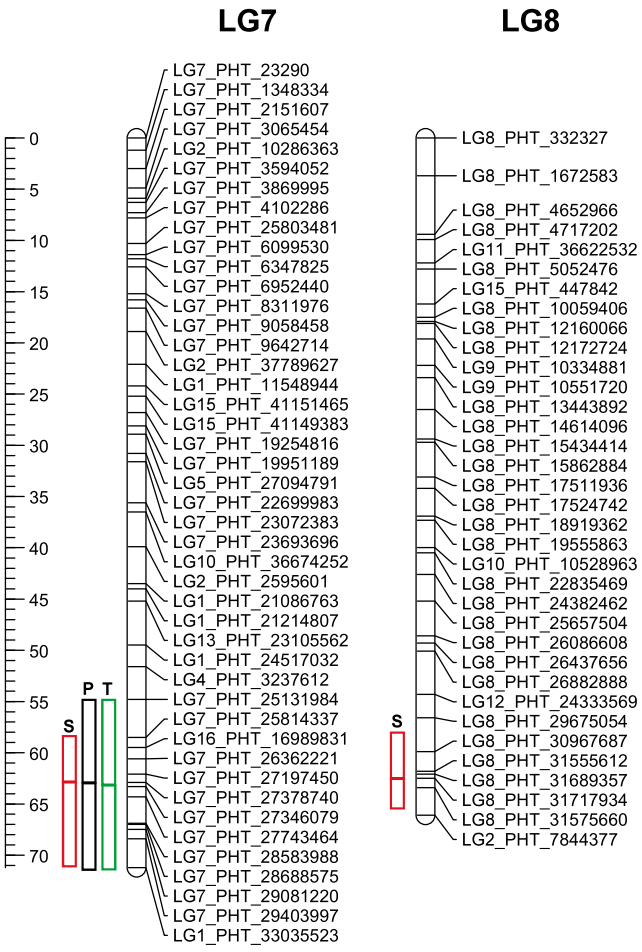

Fig. 3 Male (*M. prunifolia* PI 589816) genetic maps of linkage groups 7 and 8 from population 13,427. SNP ID refers to chromosome (LG) and its physical position determined by sequence tag alignment to the 'Golden Delicious' Whole Genome Reference Assembly v.2

DHCs are structurally similar to narigenin chalcone (a precursor to flavonols, anthocyanins, and flavan-3-ols) but, deviate early through a Δ2–3 carbon double bond reduction of *p*-coumaroyl-CoA to *p*-dihydrocoumaroyl-CoA, which is converted to phloretin through chalcone synthase (Dare et al. 2013; Ibdah et al. 2014). In phloridzin synthesis, a molecule of glucose is added to 2′-position of phloretin via phloretin 2′-O-glucosyltransferases and other glycosyltransferases (Jugdé et al. 2008; Gosch et al. 2010a). Genetic analysis identified two major determinant loci on LGs 7 and 8 for trilobatin and sieboldin, though candidate genes were not identified near these loci. The biosynthesis of sieboldin has not been elucidated, but it may form through C-3 hydroxylation of phloretin, followed by glycosylation via phloretin 4′-O-glucosyltransferase (Hutabarat et al. 2016). Although the extent of pathway sharing between sieboldin and trilobatin requires further study, dependence of sieboldin on the determinant loci on LG 7 can explain why sieboldin is not detected independent of trilobatin. As population 13,427 did not segregate for phloridzin, no determinate locus for phloridzin was detected.

In addition to phloridzin, sieboldin, and trilobatin, other DHCs are reported in *Malus*. These minor DHCs, including phloretin, generally do not occur in appreciable quantities, raising questions concerning the preferential accumulation of phloridzin, sieboldin, and trilobatin. However, in these populations, we detected an unidentified peak around 13.1 min, with maximum absorbance at 280 nm. This peak was found in similar concentrations as sieboldin or trilobatin in these populations, was strongly associated with sieboldin, and interval mapping identified a QTL for this unknown peak at the same position on LG 8. This unknown could be a hydroxylated phloretin derivative, such as hydroxyphloridzin (3-

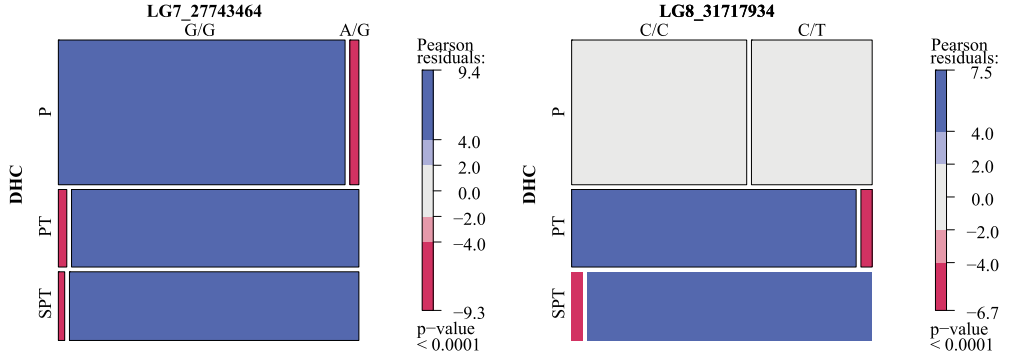

Fig. 4 Mosaic plot of proportions of dihydrochalcone (DHC) profiles by most significant SNP markers on linkage groups 7 and 8 in population 13,427. Box height represents proportion of individuals in DHC profiles and box width represents number of individuals of a genotype. Box colors represent deviation from expected observations assuming independence. Blue boxes have more individuals than expected, red boxes have fewer, and gray boxes are not significantly different based on Pearson residuals: $r_{ij} = (O_{ij}–E_{ij})/\sqrt{E_{ij}}$

hydroxyphloretin 2′-O-glucoside), but further investigation is needed.

Mean content for individual compounds varied by DHC profile, suggesting a partitioning effect among compounds. Mean phloridzin content was significantly higher in P profiles than in PT or SPT profiles, and mean trilobatin content was higher in PT profiles than in SPT profiles across all populations. Some significant positive linear relationships were observed between DHCs in some, but not all of the F_1 populations, with correlations from 0.00 to 0.74. From our observations, the correlations are stronger between trilobatin and phloridzin content when subset into PT and SPT profiles. Additionally, we observed significant variation in the proportion of DHCs relative to their parental types. While, phloridzin was the major DHC across populations, sieboldin or trilobatin were dominant in several individuals.

Chemical analysis has focused on a few key points in the DHC biosynthetic pathway. A list of key genes investigated for dihydrochalcone synthesis both in vitro and in vivo is presented in Table 6. However, cause of DHC hyper-accumulation *Malus* is unknown. Studies have shown dihydrochalcone content can be regulated via enzymes outside its biosynthetic pathway (Khan et al. 2012; Rihani et al. 2017). The evolution of trilobatin and sieboldin in select *Malus* species is of particular interest. Trilobatin differs from phloridzin by the position of the glucose moiety, which could occur through a phloretin 4′-O-glucosyltransferase (*UGT75L17*) identified on LG 9 (Yahyaa et al. 2016). Interestingly, *UGT75L17* was expressed in 'Golden Delicious', which does not accumulate trilobatin. Additionally, Dare et al. (2017) detected trilobatin accumulation after silencing phloretin 2′-O-glucosyltransferase *UGT88F1* silenced in 'Royal Gala'. These two reports highlight the biosynthetic potential for DHC synthesis beyond phloridzin in cultivated apple and emphasize the unknown mechanism for selective DHC accumulation.

The evolution of dihydrochalcone production in *Malus* is unique within the Rosaceae. Although phloretin and phloridzin are not detected in closely related pear (*Pyrus*

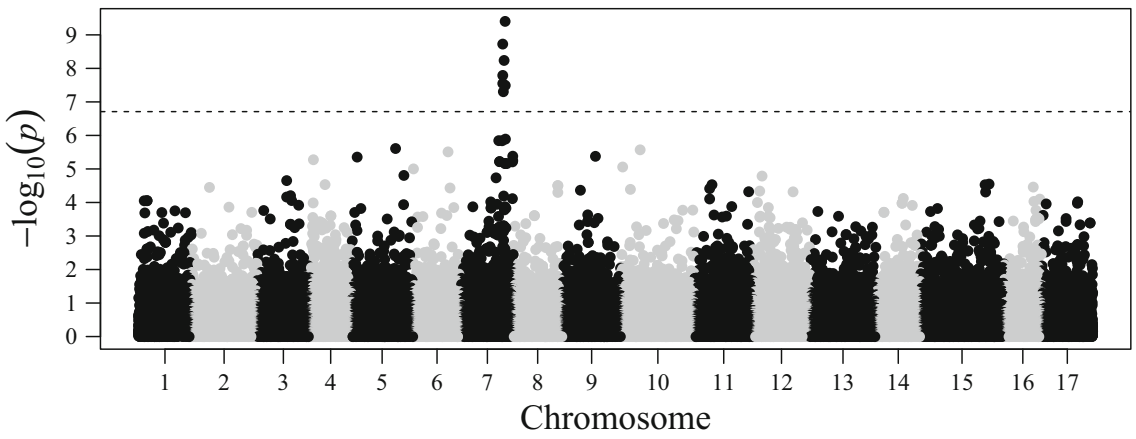

Fig. 5 Manhattan plot based on Q+K model of leaf dihydrochalcone composition in *Malus* germplasm accessions. Negative $\log_{10} p$ values are plotted by physical position on 17 apple chromosomes. Horizontal line denotes Bonferroni adjusted significance threshold at $\alpha = 0.01$

Table 6 Genes related to dihydrochalcone biosynthesis

Gene	Function	References
EU872155	Chalcone synthase	(Gosch et al. 2009; Yahyaa et al. 2017)
EU872156	Chalcone synthase	(Gosch et al. 2009; Yahyaa et al. 2017)
EU872158	Chalcone synthase	(Gosch et al. 2009; Yahyaa et al. 2017)
FJ216429	Chalcone 3-hydroxylase	(Hutabarat et al. 2016)
FJ216426	Flavonoid 3′-hydroxylase	(Hutabarat et al. 2016)
UGT88F1	Phloretin 2′-*O*-glucosyltransferase	(Gosch et al. 2010a; Dare et al. 2017)
UGT88F2	Phloretin 2′-*O*-glucosyltransferase	(Gosch et al. 2010a)
UGT71A15	Phloretin 2′-*O*-glucosyltransferase	(Jugdé et al. 2008; Gosch et al. 2012)
UGT75L17	Phloretin 4′-*O*-glucosyltransferase	(Yahyaa et al. 2016)

communis), they can be synthesized from *p*-dihydrocoumaroyl-CoA with enzymatic extracts from pear leaves, suggesting biochemical divergence in *Malus* from pear at an earlier step (Gosch et al. 2009, 2010a). Apple-pear intergeneric hybrids are able to produce both phloridzin and arbutin, a pear-specific metabolite absent in apple (Fischer et al. 2014). Although phloridzin was reported in other rosaceous plants (rose and strawberry), it is not found in high concentrations (Gosch et al. 2010b). Phloretin is the precursor to each compound, though sieboldin may be formed following an additional hydroxylation step. Phloretin was not measured in this study and is generally a minor component of dihydrochalcone content or not reported in *Malus* phenolic studies involving various tissue types (Verdu et al. 2014; Tang et al. 2015; De Paepe et al. 2015). Presumably, phloretin is nearly completely glycosylated *in planta* as it is more reactive than its glycosylated forms, resulting in cytotoxicity (Gosch et al. 2009). Silencing of *UGT88F1* in 'Royal Gala' reduced both phloridzin and phloretin, suggesting a feedback mechanism to inhibit the accumulation of phloretin in healthy plants (Dare et al. 2017).

There is evidence that phloridzin concentrations may affect other upstream pathways (Dare et al. 2017). Other QTL for DHCs have been reported in apple populations. Verdu et al. (2014) identified QTL on LGs 1 and 5 for phloridzin content in fruit and juice which explained 6.4 to 11.6% of the variation, and on LGs 3, 5, 12, and 15 for phloretin xyloglucoside content in fruit and juice which explained 17.4 to 23.6% of the variation. Chagné et al. (2012) identified a QTL for phloridzin xyloglucoside on LG 17 explaining 10.3% of the variation. No candidate genes were proposed for these reported QTL. This is the first report of DHC loci on LGs 7 and 8. Other traits mapped to LGs 7 and 8 include aphid resistance (*Dysaphis devecta* Walker and *Eriosoma lanigerum* Hausm.) (Cevik and King 2002; Bus et al. 2008); woolly apple aphid resistance allele *Er3* from *M. torigino* 'Aotea 1' (Bus et al. 2008); powdery mildew from *Malus* hybrid 'White Angel' (Evans and James 2003); fire blight resistance from 'Fiesta' (Khan et al. 2007); fruit weight (Devoghalaere et al. 2012); and fruit acidity (Zhang et al. 2012).

Conclusions

Dihydrochalcones phloridzin, sieboldin, and trilobatin are unique compounds in Malus species. We observed significant DHC content variation among five F_1 populations and segregation of DHCs in apple, following a model of three, independently segregating loci. Additionally, we identified the first genomic loci associated with trilobatin and sieboldin segregation in population 13,427 and *Malus* germplasm. Markers on LG 7 and LG 8 were strongly associated with trilobatin and sieboldin production, respectively. We posited that sieboldin is biochemically linked to trilobatin, based on the loci on LG 7. Loci identified in this study require further investigation but may facilitate the utilization of genetic resources to broaden the nutritional quality of new apple cultivars.

Acknowledgements We thank Kevin Maloney for his assistance in developing the F_1 populations. Bill Srmack and Kevin Maloney helped maintain seedlings in the greenhouses and field. Julian Koob helped prepare HPLC samples for analysis. Michael Gore, Lailiang Cheng, and Gennaro Fazio offered suggestions to improve the quality of the research and writing. BG was supported through the USDA-ARS Pathways program. JA is a participant of the ORISE-ORAU Education and Training Program.

Funding information Funding was provided by the USDA-ARS Plant Genetic Resources Unit in Geneva, NY.

Compliance with ethical standards

Conflict of interest The authors declare that they have no conflict of interest.

References

Behzad S, Sureda A, Barreca D, Nabavi SF, Rastrelli L, Nabavi SM (2017) Health effects of phloretin: from chemistry to medicine. Phytochem Rev 16:527–533

Bus VGM, Chagné D, Bassett HCM, Bowatte D, Calenge F, Celton J-M, Durel C-E, Malone MT, Patocchi A, Ranatunga AC, Rikkerink EHA, Tustin DS, Zhou J, Gardiner SE (2008) Genome mapping of three major resistance genes to woolly apple aphid (*Eriosoma lanigerum* Hausm.). Tree Genet Genomes 4:223–236

Cevik V, King GJ (2002) Resolving the aphid resistance locus *Sd-1* on a BAC contig within a sub-telomeric region of *Malus* linkage group 7. Genome 45:939–945

Chagné D, Krieger C, Rassam M, Sullivan M, Fraser J, André C, Pindo M, Troggio M, Gardiner SE, Henry RA, Allan AC, McGhie TK, Laing WA (2012) QTL and candidate gene mapping for polyphenolic composition in apple fruit. BMC Plant Biol 12:12

Danecek P, Auton A, Abecasis G, Albers CA, Banks E, DePristo MA, Handsaker RE, Lunter G, Marth GT, Sherry ST, McVean G, Durbin R (2011) The variant call format and VCFtools. Bioinformatics 27: 2156–2158

Dare A, Hellens R (2013) RNA interference silencing of *CHS* greatly alters the growth pattern of apple (*Malus* x *domestica*). Plant Signal Behav 8:e25033

Dare AP, Tomes S, Cooney JM, Greenwood DR, Hellens RP (2013) The role of enoyl reductase genes in phloridzin biosynthesis in apple. Plant Physiol Biochem 72:54–61

Dare AP, Yauk Y-K, Tomes S, McGhie TK, Rebstock RS, Cooney JM, Atkinson RG (2017) Silencing a phloretin-specific glycosyltransferase perturbs both general phenylpropanoid biosynthesis and plant development. Plant J Cell Mol Biol 91:237–250

De Paepe D, Valkenborg D, Noten B, Servaes K, Diels L, Loose MD, Van Droogenbroeck B, Voorspoels S (2015) Variability of the phenolic profiles in the fruits from old, recent and new apple cultivars cultivated in Belgium. Metabolomics 11:739–752

Devoghalaere F, Doucen T, Guitton B, Keeling J, Payne W, Ling TJ, Ross JJ, Hallett IC, Gunaseelan K, Dayatilake G, Diak R, Breen KC, Tustin DS, Costes E, Chagné D, Schaffer RJ, David KM (2012) A genomics approach to understanding the role of auxin in apple (*Malus* x *domestica*) fruit size control. BMC Plant Biol 12:7

Dong H-Q, Li M, Zhu F, Liu F-L, Huang J-B (2012) Inhibitory potential of trilobatin from *Lithocarpus polystachyus* Rehd against α-glucosidase and α-amylase linked to type 2 diabetes. Food Chem 130:261–266

Dugé de Bernonville T, Guyot S, Paulin J-P, Gaucher M, Loufrani L, Henrion D, Derbré S, Guilet D, Richomme P, Dat JF, Brisset M-N (2010) Dihydrochalcones: implication in resistance to oxidative stress and bioactivities against advanced glycation end-products and vasoconstriction. Phytochemistry 71:443–452

Dugé de Bernonville T, Gaucher M, Guyot S, Durel C-E, Dat JF, Brisset M-N (2011) The constitutive phenolic composition of two *Malus* × *domestica* genotypes is not responsible for their contrasted susceptibilities to fire blight. Environ Exp Bot 74:65–73

Elshire RJ, Glaubitz JC, Sun Q, Poland JA, Kawamoto K, Buckler ES, Mitchell SE (2011) A robust, simple genotyping-by-sequencing (GBS) approach for high diversity species. PLoS One 6:e19379

Evans K, James C (2003) Identification of SCAR markers linked to Pl-w mildew resistance in apple. Theor Appl Genet 106:1178–1183

Fan X, Zhang Y, Dong H, Wang B, Ji H, Liu X (2015) Trilobatin attenuates the LPS-mediated inflammatory response by suppressing the NF-κB signaling pathway. Food Chem 166:609–615

Fischer TC, Malnoy M, Hofmann T, Schwab W, Palmieri L, Wehrens R, Schuch LA, Müller M, Schimmelpfeng H, Velasco R, Martens S (2014) F1 hybrid of cultivated apple (*Malus* ×*domestica*) and European pear (*Pyrus communis*) with fertile F_2 offspring. Mol Breed 34:817–828

Gaucher M, Dugé de Bernonville T, Guyot S, Dat JF, Brisset M-N (2013) Same ammo, different weapons: enzymatic extracts from two apple genotypes with contrasted susceptibilities to fire blight (*Erwinia amylovora*) differentially convert phloridzin and phloretin *in vitro*. Plant Physiol Biochem 72:178–189

Glaubitz JC, Casstevens TM, Lu F, Harriman J, Elshire RJ, Sun Q, Buckler ES (2014) TASSEL-GBS: a high capacity genotyping by sequencing analysis pipeline. PLoS One 9:e90346

Gosch C, Halbwirth H, Kuhn J, Miosic S, Stich K (2009) Biosynthesis of phloridzin in apple (*Malus domestica* Borkh.). Plant Sci 176:223–231

Gosch C, Halbwirth H, Schneider B, Hölscher D, Stich K (2010a) Cloning and heterologous expression of glycosyltransferases from *Malus* x *domestica* and *Pyrus communis*, which convert phloretin to phloretin 2′-O-glucoside (phloridzin). Plant Sci 178:299–306

Gosch C, Halbwirth H, Stich K (2010b) Phloridzin: biosynthesis, distribution and physiological relevance in plants. Phytochemistry 71: 838–843

Gosch C, Flachowsky H, Halbwirth H, Thill J, Mjka-Wittmann R, Treutter D, Richter K, Hanke M-V, Stich K (2012) Substrate specificity and contribution of the glycosyltransferase UGT71A15 to phloridzin biosynthesis. Trees 26:259–271

Gutierrez BL, Zhong G-Y, Brown SK (2018) Genetic diversity of dihydrochalcone content in *Malus* germplasm. Genet Resour Crop Evol 65:1485–1502

Hunter LD (1975) Phloridzin and apple scab. Phytochemistry 14:1519–1522

Hutabarat OS, Flachowsky H, Regos I, Miosic S, Kaufmann C, Faramarzi S, Alam MZ, Gosch C, Peil A, Richter K, Hanke M-V, Treutter D, Stich K, Halbwirth H (2016) Transgenic apple plants overexpressing the *chalcone 3-hydroxylase* gene of *Cosmos sulphureus* show increased levels of 3-hydroxyphloridzin and reduced susceptibility to apple scab and fire blight. Planta 243: 1213–1224

Ibdah M, Berim A, Martens S, Valderrama ALH, Palmieri L, Lewinsohn E, Gang DR (2014) Identification and cloning of an NADPH-dependent hydroxycinnamoyl-CoA double bond reductase involved in dihydrochalcone formation in *Malus* × *domestica* Borkh. Phytochemistry 107:24–31

Jugdé H, Nguy D, Moller I, Cooney JM, Atkinson RG (2008) Isolation and characterization of a novel glycosyltransferase that converts phloretin to phlorizin, a potent antioxidant in apple. FEBS J 275: 3804–3814

Khan MA, Durel C-E, Duffy B, Drouet D, Kellerhals M, Gessler C, Patocchi A (2007) Development of molecular markers linked to the 'Fiesta' linkage group 7 major QTL for fire blight resistance and their application for marker-assisted selection. Genome 50: 568–577

Khan SA, Chibon P-Y, de Vos RCH, Schipper BA, Walraven E, Beekwilder J, van Dijk T, Finkers R, Visser RGF, van de Weg E, Bovy A, Cestaro A, Velasco R, Jacobsen E, Schouten HJ (2012) Genetic analysis of metabolites in apple fruits indicates an mQTL hotspot for phenolic compounds on linkage group 16. J Exp Bot 63: 2895–2908

Kumar S, Garrick DJ, Bink MC, Whitworth C, Chagne D, Volz RK (2013) Novel genomic approaches unravel genetic architecture of complex traits in apple. BMC Genomics 14:393–2164–14–393

Langmead B, Salzberg SL (2012) Fast gapped-read alignment with bowtie 2. Nat Methods 9:357–359

Lipka AE, Tian F, Wang Q, Peiffer J, Li M, Bradbury PJ, Gore MA, Buckler ES, Zhang Z (2012) GAPIT: genome association and prediction integrated tool. Bioinformatics 28:2397–2399

McClure KA, Sawler J, Gardner KM, Money D, Myles S (2014) Genomics: a potential panacea for the perennial problem. Am J Bot 101:1780–1790

McClure KA, Gardner KM, Toivonen PM, Hampson CR, Song J, Forney CF, DeLong J, Rajcan I, Myles S (2016) QTL analysis of soft scald in two apple populations. Hortic Res 3:16043

Mikulič Petkovšek M, Stampar F, Veberic R (2008) Increased phenolic content in apple leaves infected with the apple scab pathogen. J Plant Pathol 90:49–55

Money D, Gardner K, Migicovsky Z, Schwaninger H, Zhong G-Y, Myles S (2015) LinkImpute: fast and accurate genotype imputation for non-model organisms. G3 Genes Genomes Genet 5:2383–2390

Morimoto T, Banno K (2015) Genetic and physical mapping of *Co*, a gene controlling the columnar trait of apple. Tree Genet Genomes 11:1–11

Nair S, Ziaullah Z, Rupasinghe HV (2014) Phloridzin fatty acid esters induce apoptosis and alters gene expression in human liver cancer cells (261.2). FASEB J 28:261.2

Najafian M, Jahromi MZ, Nowroznejhad MJ, Khajeaian P, Kargar MM, Sadeghi M, Arasteh A (2012) Phloridzin reduces blood glucose levels and improves lipids metabolism in streptozotocin-induced diabetic rats. Mol Biol Rep 39:5299–5306

Orcheski B, Parker R, Brown S (2015) Pale green lethal disorder in apple (*Malus*) is caused by a mutation in the *PHYLLO* gene which is essential for phylloquinone (vitamin K1) biosynthesis. Tree Genet Genomes 11:131

Peters G-J (2018) userfriendlyscience: Quantitative analysis made accessible. R Package Version 072 Httpuserfriendlysciencecom. https://doi.org/10.17605/osf.io/txequ

Puel C, Quintin A, Mathey J, Obled C, Davicco MJ, Lebecque P, Kati-Coulibaly S, Horcajada MN, Coxam V (2005) Prevention of bone loss by phloridzin, an apple polyphenol, in ovariectomized rats under inflammation conditions. Calcif Tissue Int 77:311–318

Purcell S, Neale B, Todd-Brown K, Thomas L, Ferreira MAR, Bender D, Maller J, Sklar P, de Bakker PIW, Daly MJ, Sham PC (2007) PLINK: a tool set for whole-genome association and population-based linkage analyses. Am J Hum Genet 81:559–575

R Core Team (2016) R: a language and environment for statistical computing. R Foundation for Statistical Computing, Vienna, Austria. URL https://www.R-project.org/

Rihani KAL, Jacobsen H-J, Hofmann T, Schwab W, Hassan F (2017) Metabolic engineering of apple by overexpression of the *MdMyb10* gene. J Genet Eng Biotechnol 15:263–273

Rivière C (2016) Dihydrochalcones: occurrence in the plant kingdom, chemistry and biological activities. In: Atta-ur-Rahman (ed) Studies in natural products chemistry, 1st edn. Elsevier, pp 253–381

Slatnar A, Mikulic-Petkovsek M, Halbwirth H, Stampar F, Stich K, Veberic R (2012) Polyphenol metabolism of developing apple skin of a scab resistant and a susceptible apple cultivar. Trees 26:109–119

Tang J, Tang L, Tan S, Zhou Z (2015) The study of variation of phloridzin content in six wild *Malus* species. J Food Nutr Res 3:146–151

Verdu CF, Guyot S, Childebrand N, Bahut M, Celton J-M, Gaillard S, Lasserre-Zuber P, Troggio M, Guilet D, Laurens F (2014) QTL analysis and candidate gene mapping for the polyphenol content in cider apple. PLoS One 9:e107103

Wang Q, Tian F, Pan Y, Buckler ES, Zhang Z (2014) A SUPER powerful method for genome wide association study. PLoS One 9:e107684

Williams AH (1961) Dihydrochalcones of *Malus* species. J Chem Soc 155:4133–4136

Williams A, Jarrett J (1975) Hybridization of *Malus*. In: Report - Long Ashton Research Station 1974. University of Bristol, Bristol, p 44

Xiao Z, Zhang Y, Chen X, Wang Y, Chen W, Xu Q, Li P, Ma F (2017) Extraction, identification, and antioxidant and anticancer tests of seven dihydrochalcones from *Malus* 'Red Splendor' fruit. Food Chem 231:324–331

Yahyaa M, Davidovich-Rikanati R, Eyal Y, Sheachter A, Marzouk S, Lewinsohn E, Ibdah M (2016) Identification and characterization of UDP-glucose: phloretin 4′-O-glycosyltransferase from *Malus* x *domestica* Borkh. Phytochemistry 130:47–55

Yahyaa M, Ali S, Davidovich-Rikanati R, Ibdah M, Shachtier A, Eyal Y, Lewinsohn E, Ibdah M (2017) Characterization of three chalcone synthase-like genes from apple (*Malus* x *domestica* Borkh.). Phytochemistry 140:125–133

Yin C, Xiang L, Wang G, Wang Y, Shen X, Chen X, Mao Z (2017) Phloridzin promotes the growth of *Fusarium moniliforme* (*Fusarium verticillioides*). Sci Hortic 214:187–194

Zeileis A, Meyer D, Hornik K (2007) Residual-based shadings for visualizing (conditional) independence. J Comput Graph Stat 16:507–525

Zhang Q, Ma B, Li H, Chang Y, Han Y, Li J, Wei G, Zhao S, Khan MA, Zhou Y, Gu C, Zhang X, Han Z, Korban SS, Li S, Han Y (2012) Identification, characterization, and utilization of genome-wide simple sequence repeats to identify a QTL for acidity in apple. BMC Genomics 13:537